Structure and Chemistry of *N*-Substituted Corroles and Their Rhodium(I) and Zinc(II) Metal-Ion Complexes

Liliya Simkhovich,[a] Parameswar Iyer,[a] Israel Goldberg,*[b] and Zeev Gross*[a]

Abstract: In the present work we report on the detailed structural features of the chiral N^{21}- and N^{22}-substituted benzyl and picolyl derivatives of tris(pentafluorophenyl)corrole [H_3(tpfc)]. The main difference between the isomers is that substitution on N^{22} creates a much more crowded environment, reflected in higher deformation of the corrole ring from planarity and of the *meso*-aryls from perpendicular orientation. The effects of metal-ion chelation on corrole geometry are demonstrated by structural investigations of the zinc(II) and rhodium(I) complexes of the N^{21}- and N^{22}-alkylated corroles. The major finding is the intramolecular coordination of the pyridine moiety of the picolyl substituent in the case of [Zn^{II}(N^{21}-picolyltpfc)]. This pyridine is readily attracted to the zinc ion as an axial ligand, thus replacing the external pyridine molecule of the precursor [Zn^{II}(N^{21}-benzyltpfc)(py)]. The change is associated with a considerable flattening of the corrole ring in order to allow a more convenient coordination of the zinc ion to all four pyrrole nitrogen atoms (at Zn–N(pyrrole) distances of 1.956–1.987 Å for the nonsubstituted sites, and 2.224–2.247 Å for the substituted sites). These structural investigations also aid a good understanding of the spectroscopic characteristics of the derivatives.

Keywords: chelates · chirality · corroles · rhodium · zinc

Introduction

The chemistry of corroles and especially the development of synthetic methodologies for their preparation has a long history[1] as well as recent new horizons.[2] The original work goes back to the contributions of the Johnson group who reported the first free-base corrole in 1964 and the first *N*-substituted corroles in 1965.[3, 4] It was immediately realized that the four nitrogen atoms in corroles are not identical, that is, two isomers of *N*-substituted corroles—N^{21} and N^{22}—should be accessible.[1b, 4a] The resulting species still retain two inner NH protons and may thus be expected to form stable complexes with a variety of metal ions. This approach was pioneered by Grigg and co-workers, who demonstrated the ability of both N^{21}- and N^{22}-methylcorroles to form stable complexes with rhodium(I) and copper(II), and also reported the corresponding X-ray structures.[5] Over the years, several general trends have been observed which served to differentiate between the isomeric *N*-substituted corroles: usually the ^{1}H NMR resonances of both the NH and the NCH_2R protons are shifted to higher field for the N^{22} isomer, the electronic spectrum of the N^{21} isomer is always much more similar to that of the corrole precursor than that of the N^{22} isomer (which is red-shifted), and the N^{21} isomer is formed in excess upon alkylation of the corrole (a ratio of 1.5:1 is common). The latter two features were interpreted as an indication that the aromatic system of the N^{21} isomer is less perturbed due to less severe deviation of the macrocycle from planarity and that it is also more stable (i.e., the thermodynamic stability is also reflected in the kinetic process). These hypotheses have not been thoroughly confirmed experimentally and the NMR data have never been analyzed. The major shortcoming is the lack of crystallographic information, as until 1999 only one crystal structure of a free-base corrole had been elucidated, and there is still no structural information about any metal-free *N*-substituted corrole.[6]

We have recently reported the novel 5,10,15-tris(pentafluorophenyl)corrole (H_3(tpfc)) and many aspects of its rich chemistry.[2a, 2b, 7] This includes the facile and high-yield syntheses of its *N*-CH_2Ar-substituted (Ar = phenyl or 2-pyridyl) derivatives.[8] We have also demonstrated the chirality of these new compounds, suggesting the substitution of the N(pyrrole) sites of the corrole framework as an effective means for the synthesis of a novel class of chiral ligands. We report herein on the detailed structural features of the free-

[a] Prof. Dr. Z. Gross, Dr. L. Simkhovich, Dr. P. Iyer
Department of Chemistry and
Institute of Catalysis Science and Technology
Technion – Israel Institute of Technology
Haifa 32000 (Israel)
Fax : (+972) 4-823-3735
E-mail: chr10zg@tx.technion.ac.il

[b] Prof. Dr. I. Goldberg
School of Chemistry, Tel Aviv University
Tel Aviv 69978 (Israel)
Fax: (+972) 3-640-9293
E-mail: goldberg@chemsg7.tau.ac.il

  0947-6539/02/0811-2595 $ 20.00+.50/0

base N^{21}- and N^{22}-substituted benzyl and picolyl derivatives of H_3(tpfc). The effects of metal-ion chelation on the corrole geometry are demonstrated by structural investigations of the zinc(II) and rhodium(I) complexes with the N^{21}- and N^{22}-alkylated corroles. The study has also led to a good understanding of the spectroscopic characteristics of the derivatives.

Discussion

Structural aspects: The parent H_3(tpfc) macrocycle is already distorted from planarity by the need to accommodate the three inner protons of the corrole ring with minimal steric interference between them.[2b] Replacement of one of these protons by a much bulkier alkyl/aryl group, such as a benzyl or picolyl moiety, effects an increased hindrance inside the macrocycle and leads to severe deformation of the corrole core from planarity. This is clearly illustrated by the isomorphous structures of the N^{21}-benzyl and -picolyl structures **1** and **2** depicted in Figure 1. In the observed conformation, the N^{21} pyrrole ring is considerably tilted upward with respect to the planes of the three other pyrrole rings. Moreover, the aryl substituent on this ring is bent away from the ring in one direction, while the N^{22} and N^{24} protons are bent away in the other direction, in order to avoid collision. These deformations are best quantified by the structural parameters that are listed in Table 1. The twist angles between the planes of adjacent pyrrole rings (the individual rings are quite planar), moving around the ring from N^{21} through N^{22}, N^{23} and N^{24} to N^{21} are: 30.0, 5.9, 0.8, and 30.8° in **1** and 30.9, 5.4, 0.7, and 31.4° in **2**. These should be compared with the corresponding twist angles of 4.4, 9.4, 19.1 and 19.5° in H_3(tpfc).[2b] The deviations of the CH_2 carbon atom and the two inner protons from the plane of the three nonsubstituted pyrrole nitrogen atoms are, respectively, 1.72, −0.49, and −0.05 Å in **1** and 1.71, −0.44, and −0.51 Å in **2**. In the resulting structures, a minimal van der Waals distance of 2.2 Å is maintained between the inner NH and CH_2 protons. The aromatic substituent points upwards and towards the open space above (and parallel to) the C1−C19 bond. The three pentafluorophenyl groups are oriented roughly perpendicular to the corrole framework.

The isomorphous structures of the N^{22}-benzyl (**3**) and picolyl (**4**) derivatives are illustrated in Figure 2. They are characterized by similarly distorted conformations in which the N^{22} pyrrole that bears the bulky substituents is deflected outwards (N^{22} lies 0.43 – 0.48 Å above the plane defined by

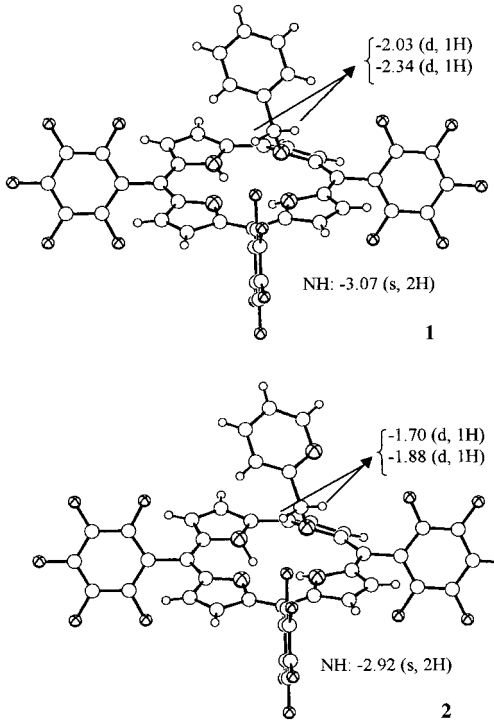

Figure 1. Molecular structures of the N^{21}-substituted corroles. Top: N^{21}-benzyl-tpfc (**1**); bottom: N^{21}-picolyl-tpfc (**2**). For clarity, in this and the following figures the various atoms are represented by arbitrarily sized spheres (detailed anisotropic displacement parameters are available in the deposited CIF files). Blank spheres represent carbon and hydrogen, while the crossed ones represent the F, N, and O heteroatoms as well as the metal ions. The numbers relate to the ^{1}H NMR chemical shifts (δ) of the relevant protons.

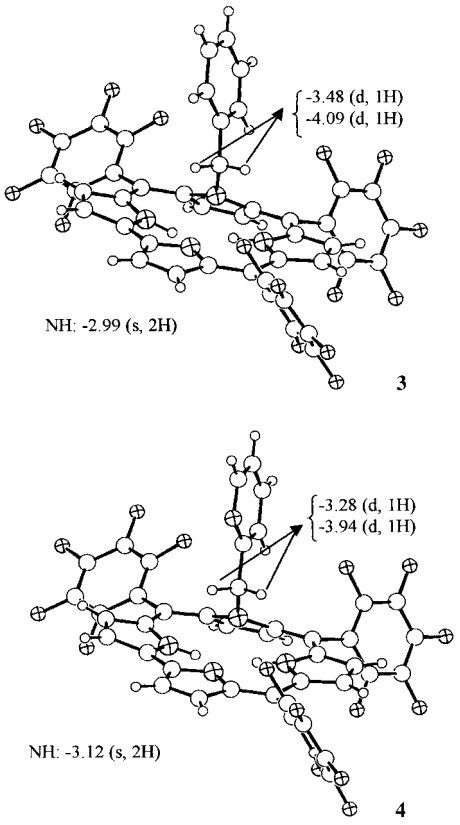

Figure 2. Molecular structures of the N^{22}-substituted corroles. Top: N^{22}-benzyl-tpfc (**3**); bottom: N^{22}-picolyl-tpfc (**4**).

Abstract in Hebrew:

בעבודה זו אנו מדווחים על התכונות המבניות של ארבעה קורולים כיראליים מותמרי חנקן. ההבדל העיקרי בין הנגזרות הוא שהתמרה על החנקן שבעמדה 22 יוצרת סביבה צפופה יותר, ענין המתבטא בעוות מוגבר של הקורול וסטיה גדולה יותר של המתמירים מהזוית האידיאלית. ממצא חשוב ביותר הוא הקואורדינציה התוך-מולקולרית של היחידה הפירידינית מתוך המתמיר הפיקולילי אל יון האבץ. המחקר המבני מוביל גם להבנה מעמיקה יותר של המאפיינים הספקטרוסקופיים של הנגזרות.

  0947-6539/02/0811-2596 $ 20.00+.50/0 *Chem. Eur. J.* **2002**, *8*, No. 11

Table 1. Selected conformation and coordination parameters (data at 110 K).

a) Free-base *N*-substituted corroles	**1**	**2**	**3**	**4**
i. Torsion angles between the pyrrole rings [°]				
N^{21} ring – N^{22} ring	30.0	30.9	34.1	32.0
N^{22} ring – N^{23} ring	5.9	5.4	36.0	34.3
N^{23} ring – N^{24} ring	0.8	0.7	4.5	3.6
N^{24} ring – N^{21} ring	30.8	31.4	10.1	10.8
ii. Deviations from the plane of the three nonsubstituted pyrrole nitrogen atoms [Å]				
substituted N	0.33	0.33	0.43	0.48
methylene C	1.72	1.71	1.78	1.81
methyl protons	1.71, 2.06	1.69, 2.05	1.83, 1.89	1.86, 1.87
inner protons	– 0.49 (H^{22})	– 0.44 (H^{22})	– 0.38 (H^{21})	– 0.31 (H^{21})
	– 0.05 (H^{24})	– 0.51 (H^{24})	0.01 (H^{23})	– 0.04 (H^{23})
iii. Dihedral angles between mean planes of the C_6F_5 substituents and the corrole carbon ring [°]				
	67.1, 68.9, 89.8	67.5, 69.0, 89.7	46.4, 50.8, 59.8	44.7, 55.8, 65.0

b) Metal complexes of *N*-substituted corroles	**5**	**6**[a]	**7**[a]
i. Torsion angles range between the pyrrole rings [°]			
N^{21} ring – N^{22} ring	33.0	30.0 – 38.8	37.4 – 43.1
N^{22} ring – N^{23} ring	36.5	1.8 – 11.1	11.7 – 17.3
N^{23} ring – N^{24} ring	35.3	2.4 – 9.5	17.1 – 22.2
N^{24} ring – N^{21} ring	31.6	36.3 – 39.7	36.7 – 38.4
ii. M – N(pyrrole) bond length range [Å] (M = Rh in **5**, Zn in **6** and **7**)	2.095 – 2.096	1.944 – 1.981	1.956 – 1.987
iii. M – N(pyrrole) nonbonding (in **5**) or weakly bonding (in **6** and **7**) distances [Å]	3.061 (N^{21})	2.382 – 2.405 (N^{21})	2.224 – 2.247 (N^{21})
	3.400 (N^{22})		
iv. M – X (axial ligand) bond lengths [Å]	1.832 (C), 2.257 (P)	2.053 – 2.085 (N_{py})	2.073 – 2.093 (N_{py})
v. Deviations from the plane of the three nonsubstituted pyrrole nitrogen atoms [Å]			
metal ion	1.51	0.55 – 0.59	0.50 – 0.51
substituted N	– 0.29	– 0.17 – – 0.30	0.41 – 0.46
methylene C	– 1.62	– 1.65 – – 1.76	1.88 – 1.92
vi. Dihedral angles between mean planes of the C_6F_5 substituents and the corrole carbon ring [°]	51.1, 58.5, 78.6	53.1, 69.4, 75.1	57.1, 71.4, 74.9
		61.1, 64.4, 82.2	62.9, 68.9, 71.1
		59.6, 72.4, 85.0	63.4, 76.5, 81.7

[a] Parameters/parameter ranges for the three independent molecules in the asymmetric unit.

the three other nitrogen atoms), while the N^{21}H protons are bent in the opposite direction to minimize repulsive interaction (Table 1). As the aromatic substituent is now located in a more crowded environment between two pentafluorophenyl groups, the detailed conformations of these compounds are slightly different from those of the former examples. The corrole ring is further deformed from planarity, and the benzyl/picolyl aryls are oriented edge-on with respect to the molecular center. The pentafluorophenyl residues are also twisted from the perpendicular orientation seen in **1** and **2** by about 20° to optimize dispersive interactions with the adjacent CH-covered fragments of these structures.

Insertion of monovalent rhodium(I), in the form of its $[Rh(CO)(PPh_3)]^+$ complex ion, into racemic **4** is associated with elimination of one of the inner protons from the corrole, and further deformation of the corrole core. As one face of the macrocycle is blocked by the picolyl substituents, the metal ion may interact only from the opposite side, the side at which the two inner protons are directed (Figure 3). In the resulting compound **5**, the rhodium ion is in a square-planar coordination environment, being ligated to the CO (at Rh–C 1.832 Å), PPh_3 (at Rh–P 2.257 Å, N^{23} and N^{24} (at Rh–N of 2.095 and 2.096 Å, respectively) sites. It is located 1.51 Å above the plane defined by the three nitrogen atoms located on this side of the corrole ring (N^{21}, N^{23}, and N^{24}). The molecular structure is further stabilized by a weak $N^{21}H\cdots N^{23}$ hydrogen bond (at H···N 2.2 Å) across the ring. The

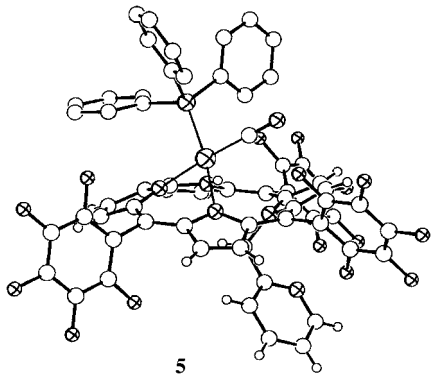

5

Figure 3. View of the molecular structure of [Rh^{I}{H(N^{22}-picolyl-tpfc)}(CO)(PPh_3)] (**5**). Hydrogen atoms on the PPh_3 residue are omitted for clarity.

observed structure of the [Rh^{I}–*rac*-(N^{22}-picolyl-tpfc)] is isomorphous with that of the corresponding [Rh^{I}–*rac*-(N^{22}-benzyl-tpfc)] isomer, reported elsewhere.[7g] Both compounds are stable towards further oxidation of the metal ion in air, preserving one inner proton within the corrole macrocycle.

Just like related porphyrin-like macrocycles, the N^{21}-aryl-tpfc ligands **1** and **2** can be also readily metallated by zinc(II). This reaction is associated with elimination of the two inner protons. Figure 4 illustrates the molecular structure of the benzyl derivative **6** crystallized in the presence of pyridine. As expected, the metal ion and the benzyl substituent on N^{21} are

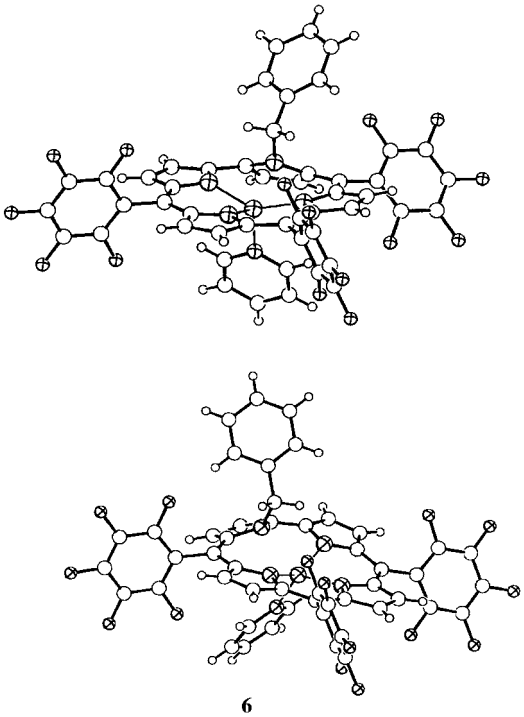

6

Figure 4. Two of the crystallographically independent enantiomers contained in the crystals of [Zn^{II}(N^{21}-benzyl-tpfc)(py)] (**6**). Note that the benzyl substituent and the pyridyl ligand are aligned in different directions with respect to the core of the corrole macrocycle.

located on opposite sides of the corrole. The zinc ion perches on one side and coordinates to the three non-alkylated pyrrole nitrogen atoms at Zn–N distances in the range of 1.944–1.981 Å. Since the N^{21} is directed at the opposite side of the corrole it may coordinate only weakly to the zinc ion (at 2.382–2.405 Å). The latter is thus forced to adopt a rather unusual pseudotrigonal coordination. This may explain its high affinity for the axial pyridyl ligand even if the latter is present in the crystallization environment only in very small amounts. As in the previous example, the axial coordination of the metal ion occurs in a direction opposite to the orientation of the benzyl substituent. For example, the zinc ion is located 0.55–0.59 Å above the plane of the three nonsubstituted nitrogen atoms, while the methylene carbon is positioned 1.65–1.71 Å below this plane. The resulting coordination geometry around the zinc ion is thus pseudotetrahedral—very uncommon for zinc complexes of porphyrins and related macrocycles. The conformation details of this corrole structure are summarized in Table 1, and are in accord with the trend observed in the previous examples. The asymmetric unit of this compound, **6**, like that of **7** (see below), contains three molecules of the complex of different chirality, allowing independent determination of the structure of the two enantiomeric species (Figure 4).

In sharp contrast to the divergent geometries of the *N*-substituted corroles and their metal complexes described above, the zinc complex of the N^{21}-picolyl-tpfc derivative represents a convergent structure (Figure 5). The pyridine moiety of the picolyl substituent is readily attracted to the zinc

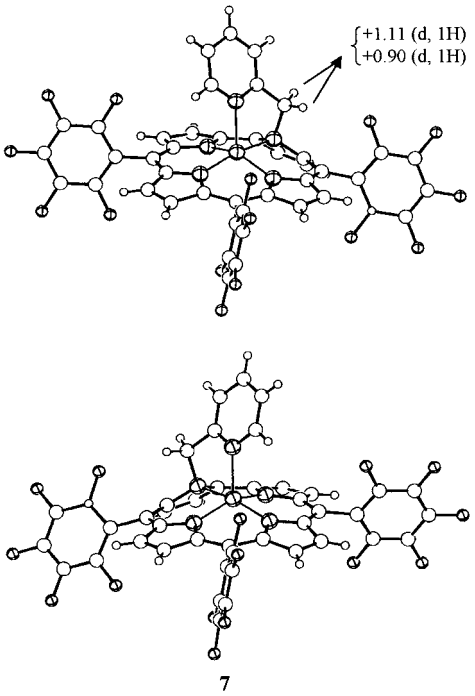

7

Figure 5. Two of the crystallographically independent enantiomers contained in the crystals of [Zn^{II}(N^{21}-picolyl-tpfc)] (**7**), illustrating the convergent arrangement of the picolyl group onto the zinc-metallated corrole and the domed structure of the latter.

ion as an axial ligand, thus replacing the external pyridine moiety of the previous example. Consequently, the corrole ring is considerably flattened in order to allow more convenient coordination of the zinc ion to all four pyrrole nitrogen atoms (at Zn–N(pyrrole) distances of 1.956–1.987 Å for the nonsubstituted sites, and 2.224–2.247 Å for the substituted sites). The strong axial coordination to the picolyl residue is reflected in the Zn–N bond lengths of 2.073–2.093 Å. The entire complex is thus characterized by a convergently domed conformation, in which the pyrrole nitrogen atoms lie about 0.25–0.44 and 0.83–0.85 Å (for N^{21}) above the plane of the 19-membered carbon macrocycle, with the zinc ion located 0.42 Å above the mean plane of the four nitrogen atoms. In this structure, the zinc ion is essentially five-coordinate with a typical (though slightly distorted) square-pyramidal geometry. It has been shown earlier that the axial coordination of the picolyl substituent can be reversibly displaced by addition of an external pyridine moiety.[8]

  0947-6539/02/0811-2598 $ 20.00+.50/0 *Chem. Eur. J.* **2002**, *8*, No. 11

Spectroscopic aspects: Another goal of the current investigations was to search for a correlation between the structural and spectroscopic features of the compounds. As far as the electronic spectra are concerned, this appears to be quite a straightforward task. The spectroscopic differences between the isomers are demonstrated in Figure 6, which compares the

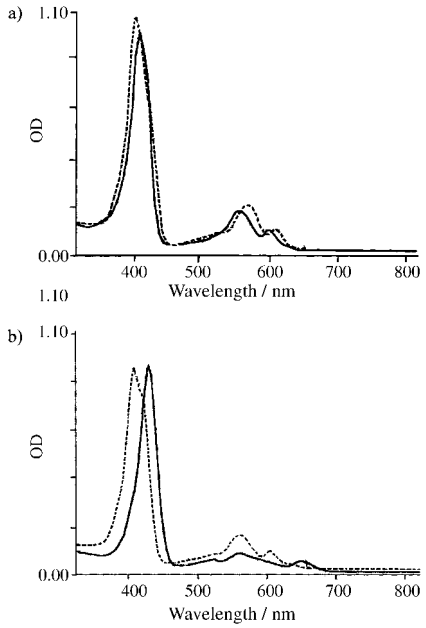

Figure 6. Electronic spectra of (top) the corrole H_3(tpfc) (broken line) and the *N*-substituted corrole **2** and (bottom) the corrole H_3(tpfc) (broken line) and the *N*-substituted corrole **4**.

spectra of **2**, **4**, and H_3(tpfc) (the spectra of **1** and **3** are very similar to those of **2** and **4**, respectively). Clearly, the spectrum of the N^{21} isomers is much more similar to that of H_3(tpfc) than to that of the N^{22} isomers, whose spectrum is shifted to significantly longer wavelengths. The crystallographic data in Table 1 show that the out-of-plane displacement of the substituted nitrogen atom in **1** and **2** is less, by about 0.1 Å, than in **3** and **4**, thus explaining the spectral similarity of the former to the nonsubstituted corrole. The significant red shift of the N^{22} isomers **3** and **4** is also in line with expectations, as extensive work on porphyrins revealed that an increase in nonplanarity is accompanied by a red shift of the electronic spectra.[9]

In the ^{1}H NMR spectra of **1**–**4** the most relevant information resides in the high-field part (between $\delta = -1$ and -4, see Figures 1 and 2), which is known to reflect the diamagnetic current effect of the aromatic macrocycle.[10] The resonances of the NH protons are found at $\delta = -3.0 \pm 0.1$ in all four compounds, consistent with the similarity of their location as deduced from their X-ray structures (Table 1 a, ii). But the N-CH_2-Ar resonances of the N^{21} isomers **1** and **2** are shifted much less (-1.7 to -2.34 ppm) than those of the N^{22} isomers **3** and **4** (-3.28 to -4.09 ppm). Attempts to use the crystallographic data per se reveal an apparent contradiction, as the distances of the substituted nitrogen atom from the plane defined by the nonsubstituted pyrrole nitrogen atoms are smaller by about 0.1 Å in **1** and **2** than those in **3** and **4** (Table 1 a ii). Accordingly, the N-CH_2-Ar resonances of **1** and **2** would be expected to be shifted more rather than less. This dilemma may be resolved by considering that while the X-ray data accounts only for one particular conformation, the NMR spectra reflect the average of all possible conformations. As may be appreciated from Figures 1 and 2 and the structural discussion, the N^{21} isomers **1** and **2** are much less crowded than the N^{22} isomers **3** and **4**. Thus, the observed conformations with the methylene protons pointing into the center of the macrocycle and the aryl group pointing away from it are less likely to be representative of the average structure in **1** and **2** than in **3** and **4**. Supporting evidence for this hypothesis is provided by the zinc(II) complex of **2** (complex **7**, Figure 5). The picolyl moiety in **7** is within the corrole center and the N-CH_2-Ar resonances are located at $\delta = 1.11$ and 0.90. The much lower likelihood of such a conformation in the N^{22} isomers is reflected in the significantly lower stability of the zinc(II) complex of **4**: all our attempts to isolate this complex failed because it liberated its metal ion very easily.

Conclusion

We have fully characterized four *N*-substituted corroles and analyzed their structural and spectroscopic aspects, as well as that of the zinc(II) and rhodium(I) complexes. It became clear that N^{21} substitution creates a less crowded environment that allows for chelation of zinc(II) to the inner core of the corrole and intramolecular binding of the picolyl subunit to the metal ion. This opens up the opportunity of utilizing such complexes—which contain both a Lewis acid and a potential nucleophile/base within a chiral environment—as catalysts for various reactions, a project that is currently under investigation in our laboratories.

Experimental Section

Physical methods: The ^{1}H NMR and ^{19}F NMR spectra were recorded on a Bruker AM 200 spectrometer, operating at 200 MHz for ^{1}H and 188 MHz for ^{19}F. Chemical shifts δ in the ^{1}H NMR spectra are reported relative to residual hydrogens in the deuterated solvents: $\delta = 7.24$ and 7.15 for chloroform and benzene, respectively, and relative to $CFCl_3$ ($\delta = 0.00$) in the ^{19}F NMR spectra. Mass spectrometry was performed on a TSQ 70 Finnigan with isobutene as carrier gas (DCI^- and DCI^+ are desorption chemical ionization methods with negative and positive detection, respectively).

Materials: Benzene (Merck, thiophene-free), for use in synthesis, was dried by distilling off a few mL. Pyridine (RDH) was dried over KOH. $[Rh_2(CO)_4Cl_2]$ (Strem), $Zn(OAc)_2 \cdot 2H_2O$ (Aldrich) and deuterated solvents (Aldrich and Cambridge Isotopes products) were used as received.

Synthetic methods: The synthetic details for the preparation of H_2(N^{21}-benzyl-tpfc) (**1**), H_2(N^{21}-picolyl-tpfc) (**2**), H_2(N^{22}-benzyl-tpfc) (**3**), and H_2(N^{22}-picolyl-tpfc) (**4**) are provided in the previous publication.[8]

(Carbon monoxide)(triphenylphosphine)rhodium(I) complex of 4 [Rh^I{H(N^{22}-picolyl-tpfc)}(CO)(PPh_3)] (5): PPh_3 (60 mg, 0.23 mmol), dry K_2CO_3 (1.56 g, 11.3 mmol), and dry NaOAc (1.85 g, 22.5 mmol) were added to **2** (20 mg, 22.6 μmol) in dry benzene (30 mL). The mixture was heated to reflux temperature under Ar and $[Rh_2(CO)_4Cl_2]$ (90 mg, 0.23 mmol) was added in portions over 3 h. After an additional 2 h under reflux (Ar atmosphere), the reaction mixture was checked by TLC (silica gel, *n*-hexane/EtOAc 10:1), confirming that all starting material had been consumed. The reaction mixture was cooled to RT and filtered, and the

solvent was evaporated. Purification of the material was performed by column chromatography (silica gel, *n*-hexane/EtOAc 100:1, only one significant fraction). A brilliant green solid was obtained after evaporation of the solvent, and X-ray quality crystals were obtained by recrystallization from benzene and *n*-heptane. The average yield of **5** for several syntheses was in the range of 60–65% (17–19 mg, 13.5–14.7 μmol). ^{1}H NMR (400 MHz, [D$_6$]benzene, RT): $\delta = 8.30$ (unresolved d, 1H; β-pyrrole H), 7.98 (m, 3H; β-pyrrole H), 7.91 (unresolved d, 1H; β-pyrrole H), 7.82 (d, $^3J(H,H) = 4.38$ Hz, 1H; β-pyrrole), 7.69 (d, $^3J(H,H) = 5.27$ Hz, 1H; β-pyrrole H), 7.47 (d, $^3J(H,H) = 4.15$ Hz, 1H; β-pyrrole H), 6.83 (t, $^3J(H,H) = 7.18$ Hz, 3H; *para*-H, PPh_3), 6.63 (t, $^3J(H,H) = 7.02$ Hz, 6H; *meta*-H, PPh_3), 5.8–6.0 (m, 9H; unresolved signals of *meta*-H (2H) and *para*-H (1H) N^{22}-pyridyl, *ortho*-H (6H) PPh_3), 3.05 (d, $^3J(H,H) = 7.77$ Hz, 1H; *ortho*-H, N^{22}-pyridyl), 1.68 (s, 1H; NH), −4.51 (d, $^3J(H,H) = 14.58$ Hz, 1H; N^{22}-pyridyl), −5.21 (d, $^3J(H,H) = 14.74$ Hz, 1H; N^{22}-pyridyl); ^{19}F NMR (188 MHz, $CDCl_3$, RT): $\delta = -136.52$ (dd, $^3J(F,F) = 23.88$ Hz, $^4J(F,F) = 8.46$ Hz, 1F; *ortho*-F); −138.114 (m, 3F; *ortho*-F); −138.84 (dd, $^3J(F,F) = 25.00$ Hz, $^4J(F,F) = 9.59$ Hz, 1F; *ortho*-F); −141.41 (dd, $^3J(F,F) = 24.064$ Hz, $^4J(F,F) = 7.76$ Hz, 1F; *ortho*-F); −153.30 (t, $^3J(F,F) = 21.056$ Hz, 1F; *para*-F); −154.169 (m, 2F; *para*-F); −161.84 (td, $^3J(F,F) = 20.68$ Hz, $^4J(F,F) = 8.46$ Hz, 1F; *meta*-F), −162.35 (td, $^3J(F,F) = 21.62$ Hz, $^4J(F,F) = 8.46$ Hz, 1F; *meta*-F), −162.71 (td, $^3J(F,F) = 22.00$ Hz, $^4J(F,F) = 8.65$ Hz, 1F; *meta*-F), −163.35 (m, 3F; *meta*-F); UV/Vis (CH_2Cl_2): λ_{max} (rel. ε, %) = 466 (100), 614 (21), 664 nm (14); MS (DCI$^-$): *m*/*z* (%): 1279 (100) $[M]^-$.

(Pyridine)zinc(II) complex of 1 [Zn^{II}(N^{21}-benzyl-tpfc)(py)] (6): Zinc acetate ($Zn(OAc)_2 \cdot 2H_2O$, 10 mg, 46 μmol) was added to a hot solution of **1** (10 mg, 11.3 μmol) in dry pyridine (2 mL), inducing an immediate color change from pink-red to green. After an additional 10 min under reflux, the solution was cooled to RT, and the pyridine was evaporated. The new green material was purified by column chromatography (silica gel, CH_2Cl_2 with a few drops of pyridine). X-ray quality crystals (17 mg, 77.3%) were obtained by recrystallization from a mixture of $CHCl_3$ and *n*-heptane. ^{1}H NMR (200 MHz, $CDCl_3$, RT): $\delta = 8.71$ (d, $^3J(H,H) = 3.8$ Hz, 1H), 8.57 (t, $^3J(H,H) = 3.77$ Hz, 2H), 8.47 (d, $^3J(H,H) = 4.9$ Hz, 2H), 8.22 (d, $^3J(H,H) = 4.4$ Hz, 1H), 7.94 (d, $^3J(H,H) = 3.6$ Hz, 1H), 6.90 (d, $^3J(H,H) = 3.89$ Hz, 1H), 6.79 (d, $^3J(H,H) = 7.22$ Hz, 1H), 6.65 (m, coordinated pyridine), 5.91 (t, $^3J(H,H) = 6.3$ Hz, 2H), 5.31 (d, $^3J(H,H) = 7.3$ Hz, 2H), −1.92 (d, $^3J(H,H) = 14.15$ Hz, 1H), −2.05 (d, $^3J(H,H) = 14.15$ Hz, 1H); ^{19}F NMR (188 MHz, $CDCl_3$, RT): $\delta = -136.56$ (dd, $^3J(F,F) = 24.25$ Hz, $^4J(F,F) = 7.52$ Hz, 1F), −137.46 (m, 2F), −137.89 (dd, $^3J(F,F) = 24.81$ Hz, $^4J(F,F) = 5.82$ Hz, 1F), −138.38 (dd, $^3J(F,F) = 24.06$ Hz, $^4J(F,F) = 7.52$ Hz, 1F), −141.66 (dd, $^3J(F,F) = 24.25$ Hz, $^4J(F,F) = 7.71$ Hz, 1F), −153.93 (t, $^3J(F,F) = 21.05$ Hz, 1F), −154.42 (t, $^3J(F,F) = 21.05$ Hz, 1F), −155.0 (t, $^3J(F,F) = 21.05$ Hz, 1F), −163.0 (m, 6F); UV/Vis (CH_2Cl_2): λ_{max} (ε) = 428 (59500), 620 nm (26700); MS (DCI$^-$): *m*/*z* (%): 948 (100) $[M]^-$.

Zinc(II) complex of 2 [Zn^{II}(N^{21}-picolyl-tpfc)] (7): This complex was prepared from compound **2** in complete analogy to the synthesis of **6** described above. $Zn(OAc)_2 \cdot 2H_2O$ (20 mg, 92 μmol) was added to a hot solution of **1** (20 mg, 22.6 μmol) in dry pyridine (5 mL). The green material (22 mg, 95%) that was obtained directly after solvent evaporation was characterized as a pentacoordinated zinc complex with external pyridine as axial ligand, [Zn^{II}(N^{21}-picolyl-tpfc)(py)]. ^{1}H NMR (200 MHz, $CDCl_3$, RT): $\delta = 8.68$ (d, $^3J(H,H) = 4.05$ Hz, 1H), 8.49 (d, $^3J(H,H) = 4.35$ Hz, 2H), 8.41 (d, $^3J(H,H) = 4.8$ Hz, 2H), 8.17 (d, $^3J(H,H) = 4.1$ Hz, 1H), 7.91 (d, $^3J(H,H) = 3.78$ Hz, 2H), 7.67 (br s, coordinated pyridine fragment of the picolyl unit), 7.11 (m, 1H), 6.79 (d, $^3J(H,H) = 4.0$ Hz, 1H), 6.65 (m, 1H), 5.51 (d, $^3J(H,H) = 7.7$ Hz, 1H), −1.41 (d, $^3J(H,H) = 13.6$ Hz, 1H), −1.53 (d, $^3J(H,H) = 13.6$ Hz, 1H); ^{19}F NMR (188 MHz, $CDCl_3$, RT): $\delta = -136.93$ (dd, $^3J(F,F) = 24.4$ Hz, $^4J(F,F) = 7.52$ Hz, 1F), −137.22 (dd, $^3J(F,F) = 24.4$ Hz, $^4J(F,F) = 7.90$ Hz, 2F), −137.97 (dd, $^3J(F,F) = 25.30$ Hz, $^4J(F,F) = 7.70$ Hz, 1F), −138.47 (dd, $^3J(F,F) = 24.80$ Hz, $^4J(F,F) = 6.80$ Hz, 1F), −142.21 (dd, $^3J(F,F) = 24.25$ Hz, $^4J(F,F) = 7.52$ Hz, 1F), −154.02 (t, $^3J(F,F) = 20.96$ Hz, 1F), −154.44 (t, $^3J(F,F) = 20.77$ Hz, 1F), −155.04 (t, $^3J(F,F) = 21.05$ Hz, 1F), −163.0 (m, 6F); UV/Vis (CH_2Cl_2): $\lambda_{max} = 428$, 620 nm. Final purification of the material was by column chromatography (silica gel, CH_2Cl_2), during which the external axial ligand (pyridine) was replaced by the intramolecular pyridine fragment of the picolyl unit. X-ray quality crystals (19 mg, 89%) were received by recrystallization from $CHCl_3$ and *n*-heptane. ^{1}H NMR (200 MHz, $CDCl_3$, RT): $\delta = 8.64$ (d, $^3J(H,H) = 4.2$ Hz, 1H), 8.48 (d, $^3J(H,H) = 5.06$ Hz, 1H), 8.34 (d, $^3J(H,H) = 4.44$ Hz, 3H), 8.27 (m, 2H), 7.62 (d, $^3J(H,H) = 3.80$ Hz, 1H), 6.72 (dt, $^3J(H,H) = 7.98$ Hz, $^4J(H,H) = 1.46$ Hz, 1H), 5.97 (t, $^3J(H,H) = 5.5$ Hz, 1H), 5.92 (d, $^3J(H,H) = 7.7$ Hz, 1H), 4.64 (d, $^3J(H,H) = 5.0$ Hz, 1H), 1.11 (d, $^3J(H,H) = 12.92$ Hz, 1H), 0.90 (d, $^3J(H,H) = 12.92$ Hz, 1H); ^{19}F NMR (188 MHz, $CDCl_3$, RT): $\delta = -137.25$ (dd, $^3J(F,F) = 24.4$ Hz, $^4J(F,F) = 8.64$ Hz, 1F), −137.84 (dd, $^3J(F,F) = 24.25$ Hz, $^4J(F,F) = 8.27$ Hz, 1F), −138.14 (dd, $^3J(F,F) = 24.44$ Hz, $^4J(F,F) = 8.46$ Hz, 1F), −138.64 (dd, $^3J(F,F) = 24.80$ Hz, $^4J(F,F) = 8.27$ Hz, 1F), −139.25 (dd, $^3J(F,F) = 24.44$ Hz, $^4J(F,F) = 8.46$ Hz, 1F), −140.28 (dd, $^3J(F,F) = 23.12$ Hz, $^4J(F,F) = 7.89$ Hz, 1F), −154.0 (t, $^3J(F,F) = 20.93$ Hz, 1F), −154.43 (t, $^3J(F,F) = 20.77$ Hz, 1F), −155.05 (t, $^3J(F,F) = 21.05$ Hz, 1F), −163.40 (m, 6F); UV/Vis (CH_2Cl_2): λ_{max} (ε) = 430 (57900), 606 nm (18600); MS (DCI$^-$): *m*/*z* (%): 949 (100) $[M]^-$.

X-ray crystallography of 1–7: The analyzed materials crystallize as solvates (with either *n*-hexane, *n*-heptane, benzene, or water), and tend to deteriorate in air. They were therefore coated with a thin layer of amorphous hydrocarbon oil in order to minimize deterioration. The X-ray diffraction measurements were carried out on a Nonius Kappa CCD diffractometer at ≈110 K in order to minimize structural disorder and thermal motion effects, and to increase the precision of the results. The crystal structures were solved by direct and Patterson methods (SIR-92, SHELXS-86, DIRDIF-96),[11] and refined by least-squares based on F^2 for all reflections (SHELXL-97).[12] All non-hydrogen atoms were refined with anisotropic displacement parameters, with the exception of those of the disordered solvent in **1** (hexane), **3** (water), and **6** (heptane), which were treated isotropically. Most of the hydrogen atoms were located in calculated positions to correspond to standard bond lengths and angles, and were included in the refinement with isotropic *U*, using a riding model; those attached to the N atoms inside the corrole ring were located in residual electron-density maps obtained from the low-temperature data. All compounds are racemic, and crystallized either in centrosymmetric space groups (**3**–**7**), or as racemic twins in a chiral space group (**1**–**2**).

H$_2$(N^{21}-benzyl-tpfc) (1), $(C_{44}H_{17}F_{15}N_4) \cdot (C_6H_{14})$: $M_r = 972.8$, monoclinic, space group $P2_1$ (No. 4), $a = 14.925(1)$, $b = 10.619(1)$, $c = 15.149(1)$ Å, $\beta = 119.39(1)^\circ$, $V = 2091.9(11)$ Å^3, $Z = 2$, $\rho_{calcd} = 1.544$ g cm^{-3}, $2\theta_{max} = 51.4^\circ$, 4167 unique reflections. Final $R1 = 0.054$ for 3581 reflections with $F > 4\sigma(F)$, $R1 = 0.068$ and $wR2 = 0.172$ for all data. Racemic twin. The hexane solvent is disordered in the lattice, and its geometry could not be reliably determined.

H$_2$(N^{21}-picolyl-tpfc) (2), $(C_{43}H_{16}F_{15}N_5) \cdot (C_7H_{16})$: $M_r = 987.8$, monoclinic, space group $P2_1$ (No. 4), $a = 15.151(1)$, $b = 10.567(1)$, $c = 15.182(1)$ Å, $\beta = 120.31(1)^\circ$, $V = 2098.4(19)$ Å^3, $Z = 2$, $\rho_{calcd} = 1.563$ g cm^{-3}, $2\theta_{max} = 51.5^\circ$, 4050 unique reflections. Final $R1 = 0.071$ for 2960 reflections with $F > 4\sigma(F)$, $R1 = 0.107$ and $wR2 = 0.177$ for all data. Racemic twin. The heptane solvent is partly disordered.

H$_2$(N^{22}-benzyl-tpfc) (3), $(C_{44}H_{17}F_{15}N_4) \cdot (H_2O)$: $M_r = 904.6$, triclinic, space group $P\bar{1}$ (No. 2), $a = 7.593(1)$, $b = 15.024(1)$, $c = 17.803(1)$ Å, $\alpha = 65.88(1)$, $\beta = 77.80(1)$, $\gamma = 85.59(1)^\circ$, $V = 1811.7(1)$ Å^3, $Z = 2$, $\rho_{calcd} = 1.658$ g cm^{-3}, $2\theta_{max} = 50.8^\circ$, 6492 unique reflections. Final $R1 = 0.048$ for 5023 reflections with $F > 4\sigma(F)$, $R1 = 0.069$ and $wR2 = 0.122$ for all data.

H$_2$(N^{22}-picolyl-tpfc) (4), $(C_{43}H_{16}F_{15}N_5) \cdot 0.5\,(C_6H_{14})$: $M_r = 930.7$, triclinic, space group $P\bar{1}$ (No. 2), $a = 7.480(1)$, $b = 15.026(1)$, $c = 18.006(1)$ Å, $\alpha = 113.48(1)$, $\beta = 96.61(1)$, $\gamma = 94.74(1)^\circ$, $V = 1825.4(1)$ Å^3, $Z = 2$, $\rho_{calcd} = 1.693$ g cm^{-3}, $2\theta_{max} = 55.9^\circ$, 8334 unique reflections. Final $R1 = 0.057$ for 5462 reflections with $F > 4\sigma(F)$, $R1 = 0.097$ and $wR2 = 0.152$ for all data. The hexane solvent is located on, and partly disordered about, centers of inversion.

[Rh^{I}{H(N^{22}-picolyl-tpfc)}(CO)(PPh_3)] (5), $(C_{62}H_{30}F_{15}N_5OPRh) \cdot 0.5\,(C_6H_6)$: $M_r = 1318.8$, monoclinic, space group $C2/c$ (No. 15), $a = 34.697(1)$, $b = 13.225(1)$, $c = 26.937(1)$ Å, $\beta = 118.58(1)^\circ$, $V = 10854.6(5)$ Å^3, $Z = 8$, $\rho_{calcd} = 1.614$ g cm^{-3}, $2\theta_{max} = 51.4^\circ$, 10087 unique reflections. Final $R1 = 0.047$ for 7067 reflections with $F > 4\sigma(F)$, $R1 = 0.083$ and $wR2 = 0.114$ for all data.

[Zn^{II}(N^{21}-benzyl-tpfc)(py)] (6), $3(C_{49}H_{20}F_{15}N_5Zn) \cdot (C_7H_{16})$: $M_r = 3187.4$, triclinic, space group $P\bar{1}$ (No. 2), $a = 14.976(1)$, $b = 18.051(1)$, $c = 27.838(1)$ Å, $\alpha = 75.61(1)$, $\beta = 77.14(1)$, $\gamma = 66.34(1)^\circ$, $V = 6612.4(1)$ Å^3, $Z = 2$, $\rho_{calcd} = 1.601$ g cm^{-3}, $2\theta_{max} = 50.6^\circ$, 23366 unique reflections. Final $R1 = 0.082$ for 13072 reflections with $F > 4\sigma(F)$, $R1 = 0.172$ and $wR2 = 0.195$ for all data. Molecules of the heptane solvent are located on, and disordered about, centers of crystallographic inversion.

0947-6539/02/0811-2600 $ 20.00+.50/0 *Chem. Eur. J.* **2002**, *8*, No. 11

[Zn^{II}(*N*^{21}-picolyl-tpfc)] (7), $3(C_{43}H_{14}F_{15}N_5Zn)\cdot(C_7H_{16})$: $M_r = 2953.1$, monoclinic, space group $P2_1/c$ (No. 14), $a = 22.603(1)$, $b = 18.117(1)$, $c = 29.387(1)$ Å, $\beta = 96.84(1)^\circ$, $V = 11984.3(3)$ Å^3, $Z = 4$, $\rho_{calcd} = 1.642$ g cm^{-3}, $2\theta_{max} = 50.7^\circ$, 20786 unique reflections. Final $R1 = 0.051$ for 14277 reflections with $F > 4\sigma(F)$, $R1 = 0.092$ and $wR2 = 0.128$ for all data.

In **6** and **7** the crystallographic asymmetric unit contains three structurally independent corrole species, one of them of different chirality from the other two. In all structures the pentafluorophenyl substituents exhibit a large-amplitude wagging motion, which reflects their partial rotational disorder.

CCDC-176178 (**1**), 176179 (**2**), 176180 (**3**), 176181 (**4**), 176182 (**5**), 176183 (**6**), and 176184 (**7**) contain the supplementary crystallographic data for this paper. These data can be obtained free of charge via www.ccdc.cam.ac.uk/conts/retrieving.html (or from the Cambridge Crystallographic Data Centre, 12 Union Road, Cambridge CB21EZ, UK; fax: (+44) 1223-336033; or deposit@ccdc.cam.uk).

Acknowledgements

This research was supported by the Israel Science foundation under Grant 368/00 and the Petroleum Research Fund (ACS). Partial support by the Mitchel Foundation and the Fund for the Promotion of Research at the Technion is acknowledged as well. P.I. thanks The Lady Davis Fellowship Trust for a postdoctoral grant.

[1] a) R. Paolesse in *The Porphyrin Handbook*, *Vol. 5* (Eds.: K. M. Kadish, K. M. Smith, R. Guilard), Academic Press, New York, **2000**, Chapter 11, pp. 201–232; b) J. L. Sessler, S. J. Weghorn in *Expanded*, *Contracted*, *and Isomeric Porphyrins* (Eds.: J. L. Sessler, S. J. Weghorn), Pergamon, Oxford, **1997**, pp. 11–125; c) A. Jasat, D. Dolphin, *Chem. Rev.* **1997**, *97*, 2267; d) E. Vogel, *J. Heterocycl. Chem.* **1996**, *33*, 1461.

[2] a) Z. Gross, N. Galili, I. Saltsman, *Angew. Chem.* **1999**, *111*, 1530; *Angew. Chem. Int. Ed.* **1999**, *38*, 1427; b) Z. Gross, N. Galili, L. Simkhovich, I. Saltsman, M. Botashansky, D. Blaser, R. Boese, I. Goldberg, *Org. Lett.* **1999**, *1*, 599–602; c) R. Paolesse, L. Jaquinod, D. J. Nucro, S. Minis, F. Sagone, T. Boschi, K. M. Smith, *Chem. Commun.* **1999**, 1307; d) D. T. Gryko, *Chem. Commun.* **2000**, 2243; e) J. W. Ka, W. S. Cho, C. H. Lee, *Tetrahedron Lett.* **2000**, *41*, 8121; f) R. Paolesse, S. Nardis, F. Sagone, R. G. Khoury, *J. Org. Chem.* **2001**, *66*, 550; g) R. P. Brinas, C. Bruckner, *Synlett* **2001**, 442; h) C. V. Asokan, S. Smeets, W. Dehaen, *Tetrahedron Lett.* **2001**, *42*, 4483; i) D. T. Gryko, K. Jadach, *J. Org. Chem.* **2001**, *66*, 4267.

[3] A. W. Johnson, I. T. Kay, *Proc. Chem. Soc.* **1964**, 89.

[4] a) A. W. Johnson, I. T. Kay, *J. Chem. Soc.* **1965**, 1620; b) A. H. Jackson, in *The Porphyrins*, *Vol. I* (Ed.: D. Dolphin), Academic Press, New York, **1979**, Chapter 8, ref. [1a], pp. 64–78.

[5] a) A. M. Abeysekera, R. Grigg, J. Trocha-Grimshaw, V. Viswanatha, T. J. King, *Tetrahedron Lett.* **1976**, 3189; b) A. M. Abeysekera, R. Grigg, J. Trocha-Grimshaw, T. J. King, *J. Chem. Soc. Perkin Trans. I* **1979**, 2184; c) R. Grigg, T. J. King, G. Shelton, *J. Chem. Soc. Chem. Commun.* **1970**, 56.

[6] H. R. Harrison, O. J. R. Hodder, D. C. Hodgkin, *J. Chem. Soc. B* **1971**, 640.

[7] a) Z. Gross, L. Simkhovich, N. Galili, *Chem. Commun.* **1999**, 599; b) L. Simkhovich, N. Galili, I. Saltsman, I. Goldberg, Z. Gross, *Inorg. Chem.* **2000**, *39*, 2704; c) A. E. Meier-Callahan, H. B. Gray, Z. Gross, *Inorg. Chem.* **2000**, *39*, 3605; d) Z. Gross, G. Golubkov, L. Simkhovich, *Angew. Chem.* **2000**, *112*, 4211; *Angew. Chem. Int. Ed.* **2000**, *39*, 4045; e) J. Bendix, G. Golubkov, H. B. Gray, Z. Gross, *Chem. Commun.* **2000**, 1957; f) J. Bendix, I. J. Dmochowski, H. B. Gray, A. Mahammed, L. Simkhovich, Z. Gross, *Angew. Chem.* **2000**, *112*, 4214; *Angew. Chem. Int. Ed.* **2000**, *39*, 4048; g) L. Simkhovich, A. Mahammed, I. Goldberg, Z. Gross, *Chem. Eur. J.* **2001**, *7*, 1041–1055; h) G. Golubkov, J. Bendix, H. B. Gray, A. Mahammed, I. Goldberg, A. J. DiBilio, Z. Gross, *Angew. Chem.* **2001**, *113*, 2190; *Angew. Chem. Int. Ed.* **2001**, *40*, 2132.

[8] Z. Gross, N. Galili, *Angew. Chem.* **1999**, *111*, 2536; *Angew. Chem. Int. Ed.* **1999**, *38*, 2366.

[9] M. O. Senge, V. Gerstung, K. Ruhlandt-Senge, S. Runge, I. Lehmann, *J. Chem. Soc. Dalton Trans.* **1998**, 4187 and references therein.

[10] C. J. Medforth, C. M. Muzzi, K. M. Shea, K. M. Smith, R. J. Abraham, S. Jia, J. A. Shelnutt, *J. Chem. Soc. Perkin Trans. 2* **1997**, 839.

[11] a) *SIR-92*: A. Altomare, M. C. Burla, M. Camalli, M. Cascarano, C. Giacovazzo, A. Guagliardi, G. Polidori, *J. Appl. Crystallogr.* **1994**, *27*, 435; b) *SHELXS-86*: G. M. Sheldrick, *Acta Crystallogr. Sect. A* **1990**, *46*, 467–473; c) P. T. Beurskens, G. Beurskens, W. P. Bosman, R. de Gelder, S. Garcia-Granda, R. O. Gould, R. Israel, J. M. M. Smits, *DIRDIF-96*, Crystallography Laboratory, University of Nijmegen (The Netherlands), **1996**.

[12] G. M. Sheldrick, *SHELXL-97*, Program for the Refinement of Crystal Structures from Diffraction Data, University of Göttingen (Germany), **1997**.

Received: December 28, 2001 [F3770]